NORMAL COMPRESSION WAVES SCATTERING AT A FLAT ANNULAR CRACK IN AN INFINITE ELASTIC SOLID*

By

YASUHIDE SHINDO

Tohoku University, Sendai, Japan

Abstract. The Hankel transform is used to obtain a complete solution for the dynamic stresses and displacements around a flat annular surface of a crack embedded in an infinite elastic solid, which is excited by normal compression waves. The singular stresses near the crack tips are obtained in closed elementary forms, while the magnitude of these stresses, governed by the dynamic stress-intensity factors, is calculated numerically from a singular integral equation of the first kind. The variations of the dynamic stress-intensity factors with the normalized frequency for the ratio of the inner radius to the outer one and Poisson's ratio are shown graphically.

1. Introduction. Since the dynamic stress-intensity factor approach of linear elastic fracture mechanics has proven to be very successful in predicting the unstable fracture of brittle solids, a good many studies of elastodynamic crack problems have been investigated [1]. Sih and Loeber [2] developed a method for examining the diffraction of torsional waves by a penny-shaped crack. The method of solution used has also been extended by Sih and Loeber [3] to solve the problem of scattering of plane-harmonic compressional and radial shear waves at a penny-shaped crack. They solved the associated integral equation numerically and obtained results which are valid at low and intermediate frequencies. Mal [4] has extended the same problems to yield information on the near field as well as the far field at any given finite frequency. These solutions were limited to two-part mixed boundary-value problems such that there was no significant difficulty involved in determining the total field at all interesting points both near to and far from the crack. On the other hand, the problem concerning a flat annular crack in an infinite elastic solid is a three-part mixed boundary-value problem, which is of considerable theoretical interest and has innumerable applications in the field of fracture mechanics as well as electromagnetic and acoustic theory. Jain and Kanwal [5] showed that the triple integral equations can be reduced to a solution of the Fredholm integral equation, and tried to solve the equation by an iterative procedure.

In a previous paper [6] we reduced the problem of diffraction of normally incident torsional waves by a flat annular crack in an elastic solid to that of finding the solution of an infinite system of simultaneous equations, and obtained numerical results for the dynamic stress-intensity factors at any given finite frequency. In this paper, the discussion is further extended to the diffraction of normal compression waves by a flat annular crack in

an elastic solid. The dynamic stresses induced by the incident waves are such that the diffraction problem is axisymmetric in character. The two surfaces of the crack are assumed to be separated by a small distance so that during small deformation of the solid, the faces do not come into contact. Hankel transform techniques and a different method analogous to that used by Erdogan [7] were adopted in the present analysis to reduce the three-part mixed boundary value problem to a singular integral equation of the first kind. Using a modification of the numerical technique described in the paper by Erdogan, Gupta, and Cook [8], we reduced the solution of the singular integral equation to that of an infinite system of simultaneous equations. The convergence of the kernel of the integral equation can be improved by means of a contour integration on the Riemann surface. Numerical calculations are carried out and the results obtained are discussed in connection with the concept of dynamic stress-intensity factor, a parameter controlling the stability or instability behavior of cracks in the theory of brittle fracture. The method of solution is such that numerical results can be obtained at any desired finite frequency.

2. Statement of the problem.   Consider a cylindrical polar coordinate system (r, θ, z) at the center of the crack as shown in Fig. 1, so that the flat annular crack is located at $z = 0$, $a \leq r \leq b$, where a and b are inner and outer radii of the crack, respectively. The displacement components in r and z directions are u_r and u_z, while the component u_θ is absent because the problem is axially symmetric. For the same reason, derivatives with respect to θ are zero. Under these conditions, the displacement components may be expressed in terms of two wave potentials $\phi(r, z, t)$ and $\psi(r, z, t)$, where t is the time, by the following relationships:

$$u_r = \phi_{,r} - \psi_{,z}, \qquad u_\theta = 0, \qquad u_z = \phi_{,z} + \psi_{,r} + \frac{\psi}{r}. \tag{1}$$

In Eqs. (1), a comma denotes partial differentiation with respect to coordinates. Substituting Eqs. (1) into Hooke's law for a homogeneous and isotropic elastic solid yields the following expressions for the stresses:

$$\sigma_{rr} = 2\mu(\phi_{,r} - \psi_{,z})_{,r} + \lambda\nabla^2\phi, \qquad \sigma_{\theta\theta} = 2\mu\frac{1}{r}(\phi_{,r} - \psi_{,z}) + \lambda\nabla^2\phi,$$

$$\sigma_{zr} = \mu\left[(2\phi_{,r} - \psi_{,z})_{,z} + \left(\psi_{,r} + \frac{\psi}{r}\right)_{,r}\right], \tag{2}$$

$$\sigma_{zz} = 2\mu\left(\phi_{,z} + \psi_{,r} + \frac{\psi}{r}\right)_{,z} + \lambda\nabla^2\phi, \qquad \sigma_{z\theta} = \sigma_{r\theta} = 0.$$
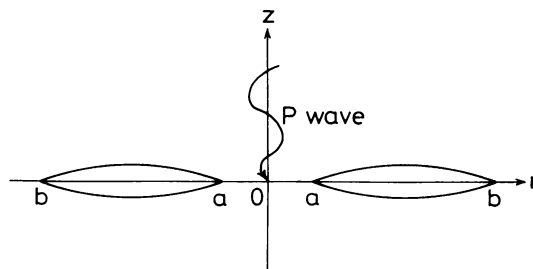

Fig. 1. Normal compression waves impinging a flat annular crack.

The symbols λ and μ stand for the Lamé constants of the elastic material and m is defined as the ratio between the shear wave velocity c_2 and the dilatational wave velocity c_1, i.e. $m = c_2/c_1$, where

$$c_1 = [(\lambda + 2\mu)/\rho]^{1/2}, \qquad c_2 = (\mu/\rho)^{1/2} \tag{3}$$

with ρ being the mass density of the elastic solid. Moreover, in Eqs. (2), ∇^2 represents the Laplacian operator in variables r and z.

By making use of Eqs. (2), the equations of motion of elasticity yield the following equations governing the potential ϕ and ψ:

$$\phi_{,rr} + \frac{1}{r}\phi_{,r} + \phi_{,zz} = \frac{1}{c_1^2}\phi_{,tt}, \qquad \psi_{,rr} + \frac{1}{r}\psi_{,r} - \frac{\psi}{r^2} + \psi_{,zz} = \frac{1}{c_2^2}\psi_{,tt}. \tag{4}$$

An incident normal compression wave can be expressed in the form:

$$u_r^{(i)} = 0, \qquad u_z^{(i)} = W_0 \exp\left[-ip\left(t + \frac{z}{c_1}\right)\right] \tag{5}$$

in which W_0 is the amplitude of the incident wave, p is the circular frequency, and a superscript i stands for the incident component. In what follows, the time factor $\exp[-ipt]$ will be omitted from all the field quantities.

The scattered portion of the solution is determined from the free crack surface condition and the symmetry property of the stress distribution, which require

$$\sigma_{zz}^{(s)}(r, 0) = -2\mu P_{10}; \qquad a < r < b, \qquad u_z^{(s)}(r, 0) = 0; \qquad r \leq a, \qquad b \leq r, \tag{6}$$

$$\sigma_{zr}^{(s)}(r, 0) = 0; \qquad r < \infty, \tag{7}$$

where $P_{10} = -i(W_0/2)(p/c_1)$ and superscript (s) stands for a scattered component.

3. Solution procedure. Application of the Hankel transform to Eqs. (4) yields

$$\phi^{(s)}(r, z) = \int_0^\infty \alpha A_1(\alpha) J_0(\alpha r) \exp[-v_1(\alpha)z] \, d\alpha; \qquad z \geq 0,$$

$$\psi^{(s)}(r, z) = \int_0^\infty \alpha A_2(\alpha) J_1(\alpha r) \exp[-v_2(\alpha)z] \, d\alpha; \qquad z \geq 0, \tag{8}$$

in which

$$v_n(\alpha) = \{\alpha^2 - (p/c_n)^2\}^{1/2} = -i\{(p/c_n)^2 - \alpha^2\}^{1/2}; \qquad n = 1, 2 \tag{9}$$

and J_0 and J_1 are, respectively, the zero and first-order Bessel functions of the first kind. The branch cuts of the function $v_n(\alpha)$ are discussed in Noble's book [9] and are not elaborated here. The unknown functions $A_1(\alpha)$ and $A_2(\alpha)$ in Eqs. (8) can be found from a system of integral equations derived from the boundary conditions.

The stress state caused by the scattering of normal compression waves from a flat annular crack is said to be symmetric if the shear stress $\sigma_{zr}^{(s)}$ vanishes on the plane $z = 0$ in which the crack is located. From the boundary conditions stated in Eqs. (6) and (7), the problem can be reduced to the solution of the triple integral equations:

$$\int_0^\infty \alpha^2 A(\alpha) J_0(\alpha r)\, d\alpha = \left[\int_0^\infty \alpha G(\alpha) J_0(\alpha r)\, d\alpha + P_{10}\right]\bigg/ (1 - m^2); \qquad a < r < b,$$

$$\int_0^\infty \alpha A(\alpha) J_0(\alpha r)\, d\alpha = 0; \qquad 0 \le r \le a, \qquad b \le r, \tag{10}$$

in which the unknown $A(\alpha)$ is related to $A_1(\alpha)$ and $A_2(\alpha)$ as follows:

$$A_1(\alpha) = \frac{1}{v_1(\alpha)} \{2(c_2\,\alpha/p)^2 - 1\} A(\alpha), \qquad A_2(\alpha) = 2\alpha(c_2/p)^2 A(\alpha) \tag{11}$$

and $G(\alpha)$ is a known function given by

$$G(\alpha) = (1 - m^2)\alpha + \frac{2}{(p/c_2)^2 v_1(\alpha)} \left[\{\alpha^2 - \tfrac{1}{2}(p/c_2)^2\}^2 - \alpha^2 v_1(\alpha) v_2(\alpha)\right]. \tag{12}$$

The set of triple integral equations (10) may be solved using a different method analogous to that used by Erdogan [7] and the result is

$$\alpha A(\alpha) = -\int_a^b t\eta(t) J_1(\alpha t)\, dt. \tag{13}$$

In Eq. (13), the function $\eta(t)$ is governed by the following singular integral equation of the first kind:

$$\frac{1}{\pi} \int_a^b \eta(t) \left[\frac{1}{r - t} + \frac{1}{2r} \log\left|\frac{2(t - r)}{(1 - a_0)b}\right| + M(r, t) + S(r, t)\right] dt = P_{10}/(1 - m^2) \tag{14}$$

satisfying the single-valuedness condition:

$$\int_a^b \eta(t)\, dt = 0. \tag{15}$$

The Fredholm kernels $M(r, t)$ and $S(r, t)$ are given

$$M(r, t) = -\frac{1}{r + t} E(r/t) + \frac{E(r/t) - 1}{r - t} - \frac{1}{2r} \log\left|\frac{2(t - r)}{(1 - a_0)b}\right|; \qquad r < t,$$

$$= \frac{1}{r + t} E(t/r) + \frac{E(r/t) - 1}{r - t} - \frac{2K(t/r)}{r} - \frac{1}{2r} \log\left|\frac{2(t - r)}{(1 - a_0)b}\right|; \qquad r > t, \tag{16}$$

$$S(r, t) = \frac{\pi t}{1 - m^2} \int_0^\infty G(\alpha) J_0(\alpha r) J_1(\alpha t)\, d\alpha. \tag{17}$$

Here, K and E are the complete elliptic integrals of the first and second kind, respectively, and $a_0 = a/b$ is the radius ratio of the annular crack.

We note that the kernel function $S(r, t)$ (Eq. (17)) is an infinite integral which has a rather slow rate of convergence. To evaluate the integral in Eq. (17), we consider the contour integrals:

$$I_{C1} = \oint_{C1} L(\xi, v_1, -v_2) J_0(\xi r) H_1^{(1)}(\xi t)\, d\xi; \qquad r < t.$$

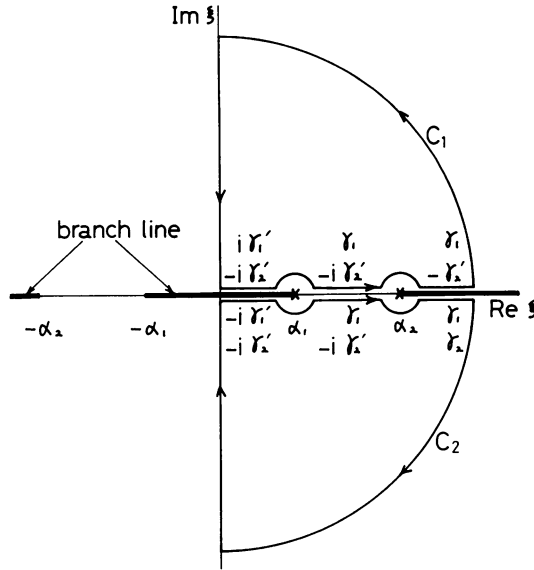$$I_{C2} = \oint_{C2} L(\xi, v_1, v_2) J_0(\xi r) H_1^{(2)}(\xi t)\, d\xi; \qquad r < t, \tag{18}$$

FIG. 2. Contours of integration for integrals in Eqs. (18).

where

$$L(\xi, v_1, v_2) = \xi + \frac{2}{(p/C_2)^2 v_2} \left[\{\xi^2 - \tfrac{1}{2}(p/C_2)^2\}^2 - \xi^2 v_1 v_2\right]. \tag{19}$$

In Eqs. (18) C_1 and C_2 stand for the contours as illustrated in Fig. 2, and $H_1^{(1)}$ and $H_1^{(2)}$ are respectively the first-order Hankel functions of the first and second kind. Letting

$$\gamma_n(\xi) = \{\xi^2 - (p/c_n)^2\}^{1/2}, \qquad \gamma'_n(\xi) = \{(p/c_n)^2 - \xi^2\}^{1/2}; \qquad n = 1, 2, \tag{20}$$

the value of v on the real ξ-axis is defined as illustrated in Fig. 2. Since $I_{c_1} + I_{c_2} = 0$, we get the relation

$$\int_{p/c_2}^{\infty} L(\xi, v_1, v_2) J_1(\xi t) J_0(\xi r)\, d\xi$$

$$= -\int_0^{p/c_1} \left[\left[\frac{2\{\xi^2 - (p/c_2)^2\}}{\gamma'_1 (p/c_2)^2} + \frac{2\xi^2 \gamma'_2}{(p/c_2)^2}\right] N_1(\xi t) + (1 - m^2)\xi J_1(\xi t)\right] J_0(\xi r)\, d\xi$$

$$- \int_{p/c_2}^{p/c_1} \left[\left[\frac{2\{\xi^2 - (p/c_2)^2\}^2}{\gamma_1 (p/c_2)^2} + (1 - m^2)\xi\right] J_1(\xi t) + \frac{2\xi^2 \gamma'_2}{(p/c_2)^2} N_1(\xi t)\right] J_0(\xi r)\, d\xi$$

$$- \frac{2}{\pi} i \int_0^{\infty} L(i\xi, i\{(p/c_1)^2 + \xi^2\}^{1/2}, \quad i\{(p/c_2)^2 + \xi^2\}^{1/2}) K_1(\xi t) I_0(\xi r)\, d\xi. \tag{21}$$

Therefore $S(r, t)$ for $r < t$ can be finally written as

$$S(r, t) = i\pi t(p/c_2)^2 \int_0^1 \frac{1}{(1 - \alpha^2)^{1/2}} \left[\tfrac{1}{2}(2m^2\alpha^2 - 1)^2 J_0(p\alpha r/c_1)H_1^{(1)}(p\alpha t/c_1)\right.$$

$$+ 2(1 - \alpha^2)\alpha^2 J_0(p\alpha r/c_2)H_1^{(1)}(p\alpha t/c_2)] \, d\alpha$$

$$- 2t(p/c_2)^2 \int_0^\infty \left[\frac{(2m^2\alpha^2 + 1)^2}{2(1 + \alpha^2)^{1/2}} - 2m^3\alpha^2(1 + m^2\alpha^2)^{1/2} - m^2(1 - m^2)\alpha\right]$$

$$\times K_1(p\alpha t/c_1)I_0(p\alpha r/c_1) \, d\alpha; \qquad r < t. \tag{22}$$

$S(r, t)$ for $r > t$ can be also found:

$$S(r, t) = i\pi t(p/c_2)^2 \int_0^1 \frac{1}{(1 - \alpha^2)^{1/2}} \left[\tfrac{1}{2}(2m^2\alpha^2 - 1)^2 H_0^{(1)}(p\alpha r/c_1)J_1(p\alpha t/c_1)\right.$$

$$+ 2(1 - \alpha^2)\alpha^2 H_0^{(1)}(p\alpha r/c_2)J_1(p\alpha t/c_2)] \, d\alpha$$

$$+ 2t(p/c_2)^2 \int_0^\infty \left[\frac{(2m^2\alpha^2 + 1)^2}{2(1 + \alpha^2)^{1/2}} - 2m^3\alpha^2(1 + m^2\alpha^2)^{1/2}\right.$$

$$- m^2(1 - m^2)\alpha]I_1(p\alpha t/c_1)K_0(p\alpha r/c_1) \, d\alpha; \qquad r > t. \tag{23}$$

In Eqs. (21)–(23), I_0, I_1, K_0 and K_1 represent the usual modified Bessel functions.

For the sake of convenience, we perform the following non-dimensionalization:

$$P = bp/c_2, \qquad R = r/b = \tfrac{1}{2}(1 - a_0)s + \tfrac{1}{2}(1 + a_0), \qquad T = t/b = \tfrac{1}{2}(1 - a_0)\tau + \tfrac{1}{2}(1 + a_0);$$

$$\Phi(\tau) = \eta(t)(1 - m^2)/P_{10}. \tag{24}$$

The revised singular integral equation of the first kind (14) and single-valuedness condition (15) are shown to be

$$\frac{1}{\pi} \int_{-1}^1 \Phi(\tau)\left[\frac{1}{s - \tau} + \frac{1 - a_0}{4R} \log|\tau - s| + \frac{1 - a_0}{2} M_0(s, \tau) + \frac{1 - a_0}{2} S_0(s, \tau)\right] d\tau = 1, \tag{25}$$

$$\int_{-1}^1 \Phi(\tau) \, d\tau = 0, \tag{26}$$

in which the Fredholm kernels $M_0(s, \tau)$ and $S_0(s, \tau)$ are

$$M_0(s, \tau) = -\frac{1}{R + T} E(R/T) + \frac{E(R/T) - 1}{R - T} - \frac{1}{2R} \log|\tau - s|; \qquad s < \tau$$

$$= \frac{1}{R + T} E(T/R) + \frac{E(T/R) - 1}{R - T} - \frac{2K(T/R)}{R} - \frac{1}{2R} \log|s - \tau|; \qquad s > \tau \tag{27}$$

$$S_0(s, \tau) = \frac{\pi T P^2}{1 - m^2} \left[i \int_0^1 \left\{\frac{(2m^2\alpha^2 - 1)^2}{2(1 - \alpha^2)^{1/2}} J_0(P\alpha Rm)H_1^{(1)}(P\alpha Tm)\right.\right.$$

$$+ 2\alpha^2(1 - \alpha^2)^{1/2}J_0(P\alpha R)H_1^{(1)}(P\alpha T)\right\} d\alpha$$

$$-\frac{2}{\pi}\int_0^\infty \left\{\frac{(2m^2\alpha^2+1)^2}{2(1+\alpha^2)^{1/2}} - 2m^3\alpha^2(1+m^2\alpha^2)^{1/2}\right.$$

$$\left. - m^2(1-m^2)\alpha\right\} K_1(P\alpha Tm)I_0(P\alpha Rm)\,d\alpha\bigg]; \qquad s < \tau$$

$$= \frac{\pi T P^2}{1-m^2}\left[i\int_0^1 \left\{\frac{(2m^2-1)^2}{2(1-\alpha^2)^{1/2}} H_0^{(1)}(P\alpha Rm)J_1(P\alpha Tm)\right.\right.$$

$$\left. + 2\alpha^2(1-\alpha^2)^{1/2}H_0^{(1)}(P\alpha R)J_1(P\alpha T)\right\} d\alpha$$

$$+ \frac{2}{\pi}\int_0^\infty \left\{\frac{(2m^2\alpha^2+1)^2}{2(1+\alpha^2)^{1/2}} - 2m^3\alpha^2(1+m^2\alpha^2)^{1/2}\right.$$

$$\left. - m^2(1-m^2)\alpha\right\} I_1(P\alpha Tm)K_0(P\alpha Rm)\,d\alpha\bigg]; \qquad s > \tau. \tag{28}$$

The solution of the singular integral equation (25) subject to the additional condition (26) can be obtained by means of the Gauss-Chebyshev integration formula. Let us expand the unknown density $\Phi(\tau)$ in the following series:

$$\Phi(\tau) = \frac{1}{(1-\tau^2)^{1/2}}\left[A_0 + \sum_{n=1}^\infty A_n T_n(\tau)\right] \tag{29}$$

where $T_n(\tau)$ are Chebyshev polynomials of the first kind and $A_n(n = 0, 1, 2, \ldots)$ are unknown constants. With Eq. (29), it follows that the condition (26) gives $A_0 = 0$. Substituting Eq. (29) into Eq. (25) and taking account of the orthogonality relations of Chebyshev polynomials [6], we finally have the following system of linear algebraic equations for the unknown constants:

$$\sum_{n=1}^\infty [\delta_{kn} + \gamma_{kn} + C_{kn}]A_n = -\delta_{1k} \tag{30}$$

where δ_{kn} is the Kronecker delta and

$$\gamma_{kn} = \frac{1-a_0}{2n\pi}\int_{-1}^1 U_{k-1}(s)(1-s^2)^{1/2}\frac{T_n(s)}{R}\,ds,$$

$$C_{kn} = -\frac{1-a_0}{\pi^2}\int_{-1}^1 U_{k-1}(s)(1-s^2)^{1/2}\,ds\int_{-1}^1 T_n(\tau)\frac{1}{(1-\tau^2)^{1/2}}$$

$$\times \{M_0(s,\tau) + S_0(s,\tau)\}\,d\tau. \tag{31}$$

In Eqs. (31), $U_n(s)$ are Chebyshev polynomials of the second kind, and all integrals are of Gauss-Chebyshev type and may easily be evaluated by using proper quadrature formulas.

4. Dynamic stress distribution around the crack. From the fracture mechanics point of view, the desired information is the stress-intensity factor which measures the load transmission of the crack. Mathematically this parameter is defined as the amplitude of the stress singularity at the tip of the crack. Thus the dynamic stress-intensity factor may be obtained by determining the stress expressions and then expanding them asymptotically around the crack tip.

Combining Eqs. (2), (8), (11), and (13), we will obtain the singular portion of the stress field by expanding the integral expressions asymptotically for large values of α and then carrying out the integration. By using the theorem [10] on the behavior of Cauchy integral near the ends of the path of integration and after some manipulations, we obtain the dynamic singular stress representations as

$$\sigma_{zz}^{(s)} \sim \frac{K_{1a}}{(2\rho_a)^{1/2}} \sin(\theta_a/2)\{1 - \cos(\theta_a/2)\cos(3\theta_a/2)\}$$

$$+ \frac{K_{1b}}{(2\rho_b)^{1/2}} \cos(\theta_b/2)\{1 + \sin(\theta_b/2)\sin(3\theta_b/2)\},$$

$$\sigma_{rz}^{(s)} \sim \frac{K_{1a}}{(2\rho_a)^{1/2}} \sin(\theta_a/2)\cos(\theta_a/2)\sin(3\theta_a/2) + \frac{K_{1b}}{(2\rho_b)^{1/2}} \sin(\theta_b/2)\cos(\theta_b/2)\cos(3\theta_b/2),$$

$$\sigma_{rr}^{(s)} + \sigma_{\theta\theta}^{(s)} + \sigma_{zz}^{(s)} \sim 2(1 + v)\left[\frac{K_{1a}}{(2\rho_a)^{1/2}} \sin(\theta_a/2) + \frac{K_{1b}}{(2\rho_b)^{1/2}} \cos(\theta_b/2)\right],$$

$$\sigma_{rr}^{(s)} - \sigma_{\theta\theta}^{(s)} \sim \frac{K_{1a}}{(2\rho_a)^{1/2}} \sin(\theta_a/2)\{1 - 2v + \cos(\theta_a/2)\cos(3\theta_a/2)\}$$

$$+ \frac{K_{1b}}{(2\rho_b)^{1/2}} \cos(\theta_b/2)\{1 - 2v - \sin(\theta_b/2)\sin(3\theta_b/2)\}, \qquad (32)$$

where K_{1a} and K_{1b} are the dynamic stress-intensity factors at the inner and the outer tips of the crack, respectively, and are defined by the following equations:

$$K_{1a} = 2\mu P_{10} b^{1/2}\left(\frac{1 - a_0}{2}\right)^{1/2} \sum_{n=1}^{\infty}(-1)^n A_n,$$

$$K_{1b} = -2\mu P_{10} b^{1/2}\left(\frac{1 - a_0}{2}\right)^{1/2} \sum_{n=1}^{\infty} A_n. \qquad (33)$$

In Eqs. (32), (ρ_a, θ_a) and (ρ_b, θ_b) are the polar coordinates defined as

$$\rho_a = \{(r - a)^2 + z^2\}^{1/2}, \qquad \theta_a = \tan^{-1}\left\{\frac{z}{r - a}\right\},$$

$$\rho_b = \{(r - b)^2 + z^2\}^{1/2}, \qquad \theta_b = \tan^{-1}\left\{\frac{z}{r - b}\right\}. \qquad (34)$$

5. Numerical results and discussion. Numerical results have been calculated for the dynamic stress-intensity factor as a function of the normalized frequency P with various ratios of a_0. The infinite system of simultaneous equations (30) is solved by an approximate method in which only the first N equations containing only the first N unknowns are taken. In the calculated results, it is found that the value of N needed to achieve a particular level of accuracy is strongly dependent on a_0 and the truncation after $N = 16, 12, 10, 8$ and 6 gives practically adequate results at any desired finite frequency for $a_0 = 0.1, 0.3, 0.5, 0.7$ and 0.9, respectively. As the wavelength of the incident compressional wave becomes very long, P approaches zero and the dynamic stress-intensity factor K_{1b} at the outer tip of the crack in the case of $a_0 = 0$ simplifies to the static solution $K_{1s} = (4/\pi)\mu P_{10} b^{1/2} \cdot K_{1s}$ denotes the stress-intensity factor for the infinite solid with a penny-shaped crack of radius b and the dynamic stress-intensity factors are normalized by K_{1s}.
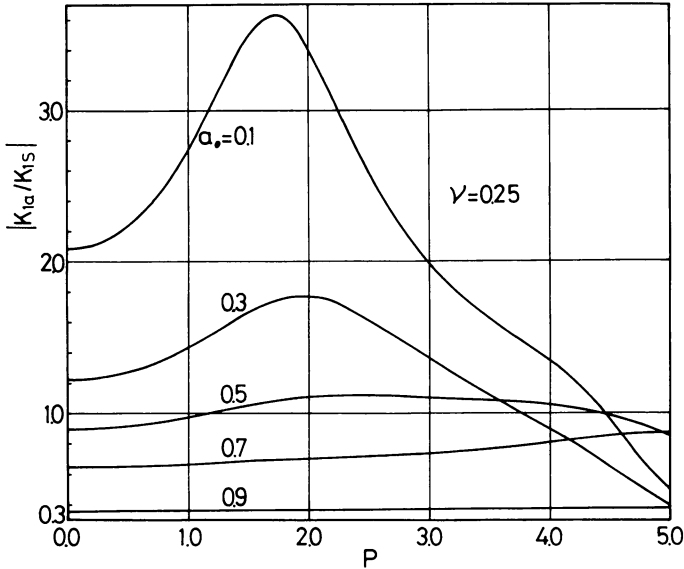
FIG. 3. Dynamic stress-intensity factors at the inner tip of the crack versus P.

Graphs of $|K_{1a}/K_{1s}|$ plotted against P for $a_0 = 0.1, 0.3, 0.5, 0.7, 0.9$ and a Poisson's ratio of 0.25 are shown in Fig. 3. $|K_{1a}/K_{1s}|$ becomes very large as $a_0 \to 0$ and tends to zero as $a_0 \to 1$. The same kind of results for $|K_{1b}/K_{1s}|$ are shown in Fig. 4, in which the dashed curve is the result for the case of penny-shaped crack by Mal [4]. $|K_{1b}/K_{1s}|$ tends to the result for a penny-shaped crack as $a_0 \to 0$ and tends to zero as $a_0 \to 1$. When a_0 tends to 1.0, both $|K_{1a}/K_{1s}|$ and $|K_{1b}/K_{1s}|$ approach to the normalized dynamic stress-intensity factor for a Griffith crack of length $b - a$ in the plane strain state. As P approaches zero, $|K_{1a}/K_{1s}|$ and $|K_{1b}/K_{1s}|$ tend to the static solutions for the annular crack, respectively.
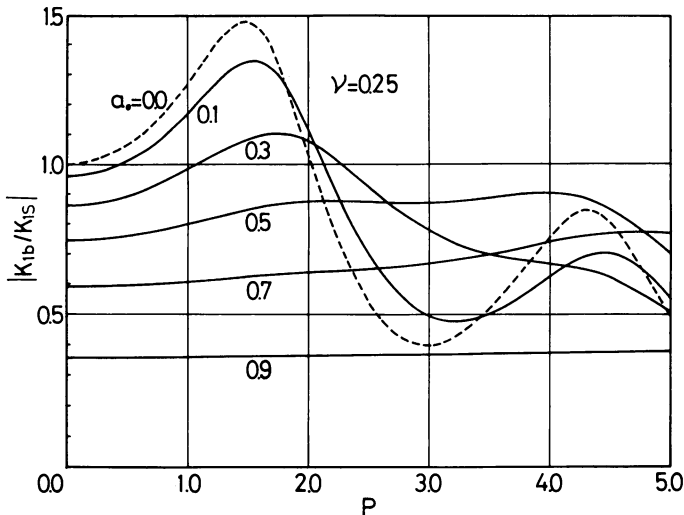

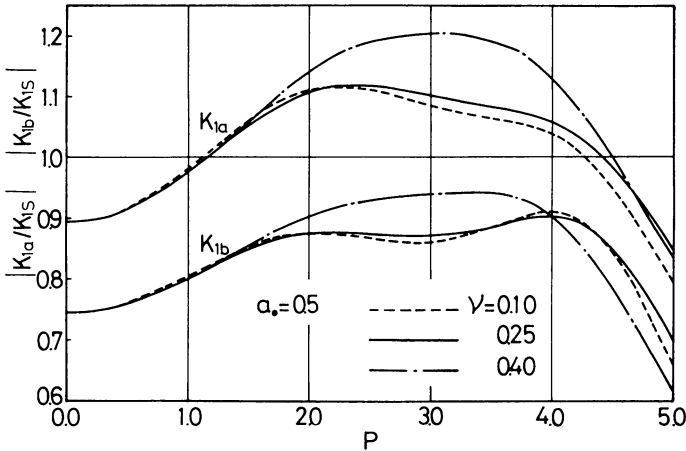FIG. 4. Dynamic stress-intensity factors at the outer tip of the crack versus P.

FIG. 5. Effect of Poisson's ratio on K_{1a} and K_{1b} factors for $a_0 = 0.5$.

Similar results in the static case have been already obtained by Shibuya, Nakahara, and Koizumi [11]. Some of their results are not in agreement with the results obtained here. This may have been caused by the computational difficulties in the evaluation of the improper integrals. The results of good accuracy are obtained in the present case. Numerical results for the case $a_0 = 0.1, 0.3, 0.5, 0.7, 0.9$ and $v = 0.25$ show that $|K_{1a}/K_{1s}|$ is always larger than $|K_{1b}/K_{1s}|$ in the range of $0 \le P \le 4.6$. It follows from this that the form of the annular crack is unstable for the range. And then the development of the crack for a monotonic increase of the vibrating load P_{10} applied at infinity starts at points of the inner tip and the annular crack transforms into a penny-shaped crack of radius b. The maximum value of the dynamic stress-intensity factor for a penny-shaped crack exceeds the corresponding static value by 48% [4]. From the present numerical results, the maximum values of $|K_{1a}/K_{1s}|$ and $|K_{1b}/K_{1s}|$ for $a_0 = 0.1$ and $v = 0.25$ are 75% and 41% larger than the static values, respectively. Unlike the case of the torsional problem [6], the maximum value of $|K_{1a}/K_{1s}|$ at $a_0 = 0.1, 0.3, 0.5, 0.7, 0.9$ is always larger than that of $|K_{1b}/K_{1s}|$, and is produced at higher frequencies than that except $a_0 = 0.5$. As a_0 increases, the maximum of $|K_{1a}/K_{1s}|$ and $|K_{1b}/K_{1s}|$ is shifted to the higher frequencies and decreases. The variations of $|K_{1a}/K_{1s}|$ and $|K_{1b}/K_{1s}|$ with P become gentle as a_0 increases.

Exhibited in Fig. 5 is the effect of Poisson's ratio v on the values of the $|K_{1a}/K_{1s}|$ and $|K_{1b}/K_{1s}|$ curves for $a_0 = 0.5$. The curves for K_{1a} show that larger values of v produce greater peak values. Note that the changes in Poisson's ratio have a greater influence on the graphs.

REFERENCES

[1] G. C. Sih, *Elastodynamic crack problems*, Noordhoff International Publishing, Leyden, 1977
[2] G. C. Sih and J. F. Loeber, *Torsional vibration of an elastic solid containing a penny-shaped crack*, J. Acoust. Soc. Amer. **44**, 1237–1245 (1968)
[3] G. C. Sih and J. F. Loeber, *Normal compression and radial shear waves scattering at a penny-shaped crack in an elastic solid*, J. Acoust. Soc. Amer. **46**, 711–721 (1969)
[4] A. K. Mal, *Interaction of elastic waves with a penny-shaped crack*, Int. J. Engng. Sci. **8**, 381–388 (1970)
[5] D. L. Jain and R. P. Kanwal, *An integral equation method for solving mixed boundary value problems*, SIAM J. Appl. Math. **20**, 642–658 (1971)

[6] Y. Shindo, *Diffraction of torsional waves by a flat annular crack in an infinite elastic medium*, J. Appl. Mech. **46**, 827–831 (A79)

[7] F. Erdogan, *Stress distribution in bonded dissimilar materials containing circular or ring-shaped cavities*, J. Appl. Mech. **32**, 829–836 (1965)

[8] F. Erdogan, G. D. Gupta and T. S. Cook, *Methods of analysis and solutions of crack problems*, Noordhoff International Publishing, Leyden, 1973, p. 368

[9] B. Noble, *Methods based on the Wiener-Hopf technique*, Pergamon Press Inc., New York, 1958

[10] N. I. Muskhelishvili, *Singular integral equations*, Noordhoff, Groningen, 1946

[11] T. Shibuya, I. Nakahara and T. Koizumi, *The axisymmetric distribution of stresses in an infinite elastic solid containing a flat annular crack under internal pressure*, ZAMM **55**, 395–402 (1975)